

# Dual Sliding Statistics Switching Median Filter for the Removal of Low Level Random-Valued Impulse Noise

M. H. Suid<sup>†</sup>, M. F. M. Jusof\* and M. A. Ahmad\*

**Abstract** – A new nonlinear filtering algorithm for effectively denoising images corrupted by the random-valued impulse noise, called dual sliding statistics switching median (DSSSM) filter is presented in this paper. The proposed DSSSM filter is made up of two subunits; i.e. Impulse noise detection and noise filtering. Initially, the impulse noise detection stage of DSSSM algorithm begins by processing the statistics of a localized detection window in sorted order and non-sorted order, simultaneously. Next, the median of absolute difference (MAD) obtained from both sorted statistics and non-sorted statistics will be further processed in order to classify any possible noise pixels. Subsequently, the filtering stage will replace the detected noise pixels with the estimated median value of the surrounding pixels. In addition, fuzzy based local information is used in the filtering stage to help the filter preserves the edges and details. Extensive simulations results conducted on gray scale images indicate that the DSSSM filter performs significantly better than a number of well-known impulse noise filters existing in literature in terms of noise suppression and detail preservation; with as much as 30% impulse noise corruption rate. Finally, this DSSSM filter is algorithmically simple and suitable to be implemented for electronic imaging products.

**Keywords:** Image processing, Random-valued impulse noise, Digital image, Nonlinear noise filtering.

## 1. Introduction

In the era of multimedia technology, the use of digital image-based visual information has gained a lot of attention due to its flexibility and this phenomenon is expected to continue growing. Medical imaging diagnosis and geographical analysis are among modern daily life applications which have adopted digital image processing technology. In general, these applications involve numerous image processing operations (e.g. image segmentation, edge detection, classification, etc.) of which are highly dependent on the quality of digital input images in order for them to work perfectly. Unfortunately, digital images are frequently subjected to the contamination of impulse noise that typically due to the interferences generated during transmission/acquisition or storage through electronic medium [1]. Therefore, it is imperative to remove the impulse noise effect before any subsequent image processing operations can be carried out as the occurrences of impulse noise can severely damage the information in the original image. One of the most effective approaches to cater for the occurrence of impulse noise and for the improvement of the quality of the acquired image is by using denoising-based algorithm. Accordingly, a large number of nonlinear filters have been widely exploited to remove the impulse noise as they are generally more superior to linear filtering

techniques. For instance, standard median (SM) filter [2] and adaptive median (AM) filter [3] are two of the most basic nonlinear filtering techniques for suppressing impulse noise. Ironically, this SM is implemented unconditionally across the image while its variants (e.g. see AM) inherited this clumsy smoothing property; thus they tend to modify both noise and noise-free pixels simultaneously. Consequently, the detailed regions such as object edges and fine textures in image are smeared and appear blurry or jittered.

To get rid of the problem, various filters under switching scheme have been studied and experimented by a number of recently published works; such as switching median filter I and II (SWM-I and SWM-II) [4], multi-state median (MSM) filter [5], Laplacian switching median (LSM) filter [6], enhanced rank impulse detector (ERID) [7], directional weighted median (DWM) filter [8] and noise-ranking switching filter (NRSF) [9], etc. Basically, this filtering scheme divides its implementation into two stages; which are impulse noise detection stage and impulse noise filtering stage. Impulse noise detection algorithm is implemented prior to the filtering process in order to determine whether a pixel should be modified or left unchanged. With this kind of filtering properties, these techniques are shown to be more effective to preserve most of the image details compared to the conventional non-switching techniques.

In a different way, Chen and Wu [10] have come out with the technique based on the adaptive switching scheme called adaptive center-weighted median (ACWM) filter. Briefly, ACWM is a two phase iterative median filter

<sup>†</sup> Corresponding Author: Faculty of Electrical and Electronic Engineering, Universiti Malaysia Pahang, Malaysia. (mhelmi@ump.edu.my)

\* Faculty of Electrical and Electronic Engineering, Universiti Malaysia Pahang, Malaysia. (mfalfazli@ump.edu.my)

Received: April 28, 2016; Accepted: January 22, 2018

which uses a fixed processing window size with adaptively filtering process. Apart from the switching scheme and the adaptive switching scheme, the hybrid switching scheme is another class of filters which has been groomed to yield good filtering results. Many researchers have embedded other order statistics (e.g. rank-order statistic, median of absolute deviations, etc.) and image processing techniques (e.g. mathematical morphology, directional or edge detection, etc.) into the hybrid switching scheme filters as part of its filtering mechanism. One of the techniques in this filtering scheme is the work done by Chen et al. [11]. In general, this tri-state median (TSM) filter is formed by a combination of SM and center weighted median (CWM) filter [12]. It uses a set of two predefined thresholds to determine whether the original pixel should be retained or replaced by the SM filtered output or the CWM filtered output. Meanwhile, a more sophisticated filtering technique has been presented by Luo in [13]. This filter incorporates the rank order absolute difference (ROAD) statistics with fuzzy impulse detection algorithm to classify and remove impulse noise from corrupted images. Noticeably, the restoration abilities of those aforementioned techniques are improved but at the cost of lost fine image details and increased complexity.

Of late, in accordance with the evolution in digital image acquisition technologies, the corruption rate of impulse noise in digital images has managed to be reduced to the level that may be regarded as low; i.e. less than 30% noise density [14-17]. Based on the aforementioned statements and observations; hence our aim in this paper is to develop an efficient filtering technique with a reasonable processing time, particularly for the range of low level impulse noise. Towards this, we introduce a new iterative and recursive filter known as dual sliding statistics switching median (DSSSM). This proposed filter is relatively fast and can remove the impulse noise dexterously without jeopardizing the details and textures inside the image.

The organization of this paper is as follows. Section 2 discusses on the impulse noise model. The design of the proposed filter is described in Section 3. Simulations and experimental results are presented in Section 4. Finally a brief conclusion is drawn in Section 5.

## 2. Impulse Noise Model

Theoretically, impulse noise contaminates an image with a random amplitude which could either fall within the image dynamic range (i.e. random-valued impulse noise) or out of the range (i.e. salt-and-pepper noise), and usually only certain percentage of pixels are affected. In this work, we tend to focus on the random-valued impulse noise and the model of this impulse noise is described for clarity. For detail, let  $x(i, j)$  and  $o(i, j)$  be the gray level of the noisy image and the original image at location  $(i, j)$ , respectively. Then, the impulse noise model with noise density  $r$  can be

defined as:

$$x(i, j) = \begin{cases} n(i, j) & : \text{with probability } r \\ o(i, j) & : \text{with probability } 1-r \end{cases} \quad (1)$$

where  $n(i, j)$  is the noise pixel value independent from  $o(i, j)$ . The image is said to be corrupted by the random-valued impulse noise when  $n(i, j)$  uniformly distributed within the image dynamic range, i.e.  $n(i, j) \in [N_{\min}, N_{\max}]$ . For example, in an 8-bit gray scale image with 256 gray levels, the  $n(i, j)$  may range from 0 ( $N_{\min}$ ) to 255 ( $N_{\max}$ ).

In practical, identifying this noise is more challenging compared to the salt-and-pepper noise because the intensity of noisy pixel is very similar to its surrounding [18-20].

## 3. Dual Sliding Statistics Switching Median Filter

Dual sliding switching median (DSSSM) filter is an iterative nonlinear filter which consists of two processing stages. The first stage involves the detection of impulse noise and its location. A noise mask, acting as a classifier to separate the noise pixels from noise-free pixels is generated during this process. In the second stage, all noise-free pixels are left uncorrected while the other noise pixels will be subjected for further processing. At this level, the pixel restoration process is carried out recursively with the assistance of fuzzy based local information. The mechanism of the proposed DSSSM filter is discussed and explicated with more specific in the following subsections.

### 3.1 Stage 1: Impulse noise detection

In digital image, the noisy pixel can be characterized by a pixel with the intensity that varies greatly from those of its neighboring pixels. Basically, the intensities of these pixels are represented by a numerical integer. Based on this fact, the impulse detection can be realized by analyzing the local image statistics within a window patch. In the beginning of the detection process, the proposed DSSSM filter employs a square local window  $W(i, j)$  with odd dimensions  $(2N+1) \times (2N+1)$  and is centered at  $x(i, j)$ . It is given as:

$$W(i, j) = \{x(i+k, j+l)\}; \text{ where } \begin{matrix} k, l \in \{-N, \dots, 0, \dots, N\} \end{matrix} \quad (2)$$

All the pixel's elements within  $W(i, j)$  are then stored in two separate arrays which represent the sorted statistics and non-sorted statistics, respectively. The process is continued by finding the median pixel  $P_{med}(i, j)$  and central pixel  $P_{center}(i, j)$ . Both  $P_{med}(i, j)$  and  $P_{center}(i, j)$  are defined by:

$$P_{med}(i, j) = \text{med}\{x(i+k, j+l)\} \quad (3)$$

$$P_{center}(i, j) = x(i, j) \quad (4)$$

Next, the median pixel  $P_{med}(i, j)$  and central pixel  $P_{center}(i, j)$  are subtracted from all the pixels in  $W(i, j)$ . This modulus operandi will produce two sets of absolute differences arrays, namely  $d_{med}(i+k, j+l)$  and  $d_{center}(i+k, j+l)$ . Mathematically, these absolute differences arrays are computed as follows:

$$d_{med}(i+k, j+l) = |x(i+k, j+l) - P_{med}(i, j)|; \text{ with } k, l \neq 0 \quad (5)$$

$$d_{center}(i+k, j+l) = |x(i+k, j+l) - P_{center}(i, j)|; \text{ with } k, l \neq 0 \quad (6)$$

At this point, all the values computed in  $d_{med}(i+k, j+l)$  and  $d_{center}(i+k, j+l)$  are rearranged in ascending order. After that, the median of absolute differences (i.e.  $MAD_{med}$  and  $MAD_{center}$ ) will be identified based on:

$$MAD_{med} = \text{med}\{d_{med}(i+k, j+l)\} \quad (7)$$

$$MAD_{center} = \text{med}\{d_{center}(i+k, j+l)\} \quad (8)$$

In order to make a distinction whether current processing pixel is a noise or not, the difference between  $MAD_{med}$  and  $MAD_{center}$  will be first calculated. If the MAD difference is denoted as  $diffMAD$ , then alternatively  $diffMAD$  can be written as follows:

$$diffMAD = |MAD_{med} - MAD_{center}| \quad (9)$$

This  $diffMAD$  provides information about the likelihood of corruption for the current processing pixel. For example, if  $diffMAD$  value is large then the current pixel is very likely being contaminated by impulse noise. On the other hand, in the case where  $diffMAD$  is small, the current pixel may be considered as a noise-free.

After  $diffMAD$  is counted, a binary noise mask  $M(i, j)$  will be formed to mark the locations of noise pixels and noise-free pixels. Thus, the process of generating noise mask can be grasped as:

$$M(i, j) = \begin{cases} 1, & diffMAD > T^{(t)}_{DSSSM} \\ 0, & diffMAD \leq T^{(t)}_{DSSSM} \end{cases} \quad (10)$$

where  $M(i, j)=1$  signifies the noise pixel,  $M(i, j)=0$  represents the noise-free pixel and  $T^{(t)}_{DSSSM}$  actually is the threshold in the t-th iteration.

### 3.2 Stage 2: Noise filtering

After the binary noise mask is created, the filtering action will replace the noise pixels marked with  $M(i, j)=1$  with the estimated correction term. Yet again, the proposed DSSSM filter adopts a square sliding window  $W_{filter}(i, j)$

with  $(2N_{filter}+1) \times (2N_{filter}+1)$  dimensions. The so called filtering window is given as:

$$W_{filter}(i, j) = \{x(i+k, j+l)\}; \text{ where } k, l \in (-N_{filter}, \dots, 0, \dots, N_{filter}) \quad (11)$$

For each detected noise pixel, the median pixel  $m(i, j)$  is selected from the corresponding region within  $W_{filter}(i, j)$  using:

$$m(i, j) = \text{med}\{x(i+k, j+l)\} \quad (12)$$

Then, the local information  $D_{local}(i, j)$  is extracted from  $W_{filter}(i, j)$  according to:

$$D_{local}(i, j) = \max |x(i+k, j+l) - x(i, j)|; \text{ with } (i+k, j+l) \neq i, j \quad (13)$$

As part of the filtering mechanism in the DSSSM filter, fuzzy reasoning is applied to the extracted local information. The fuzzy set will handle any uncertainties present in the local information due to the nonlinear nature of impulse noise corrupting an image. This adopted fuzzy set  $f(i, j)$  is defined by:

$$f(i, j) = \begin{cases} 0 & : D_{local}(i, j) < T_1 \\ \frac{D_{local}(i, j) - T_1}{T_2 - T_1} & : T_1 \leq D_{local}(i, j) < T_2 \\ 1 & : D_{local}(i, j) \geq T_2 \end{cases} \quad (14)$$

where  $T_1$  and  $T_2$  are two empirically predefined threshold with the value 10 and 30 respectively. Finally, the correction term  $y_{DSSSM}(i, j)$  is used to replace the detected noise pixel. It will utilize the median pixel  $m(i, j)$  and fuzzy set  $f(i, j)$  obtained in two previous processes. The correction term is computed as follows:

$$y_{DSSSM}(i, j) = [1 - f(i, j)] \cdot x(i, j) + f(i, j) \cdot m(i, j) \quad (15)$$

As to enhance the filter's ability in selecting a more accurate median pixel, this algorithm is implemented in recursive manner. An illustrative example of the impulse noise detection and filtering operation against an image with the corruption rate of 10% is shown in Fig. 1.

### 3.3 The selection of the parameters

Generally, the selection of threshold set and number of iterations needed for every level of noise density are essential since it will influence the performance of the proposed filter. In this framework, we have fixed the number of iterations based on the impulse noise density. By taking into account the trade-off between good filtering

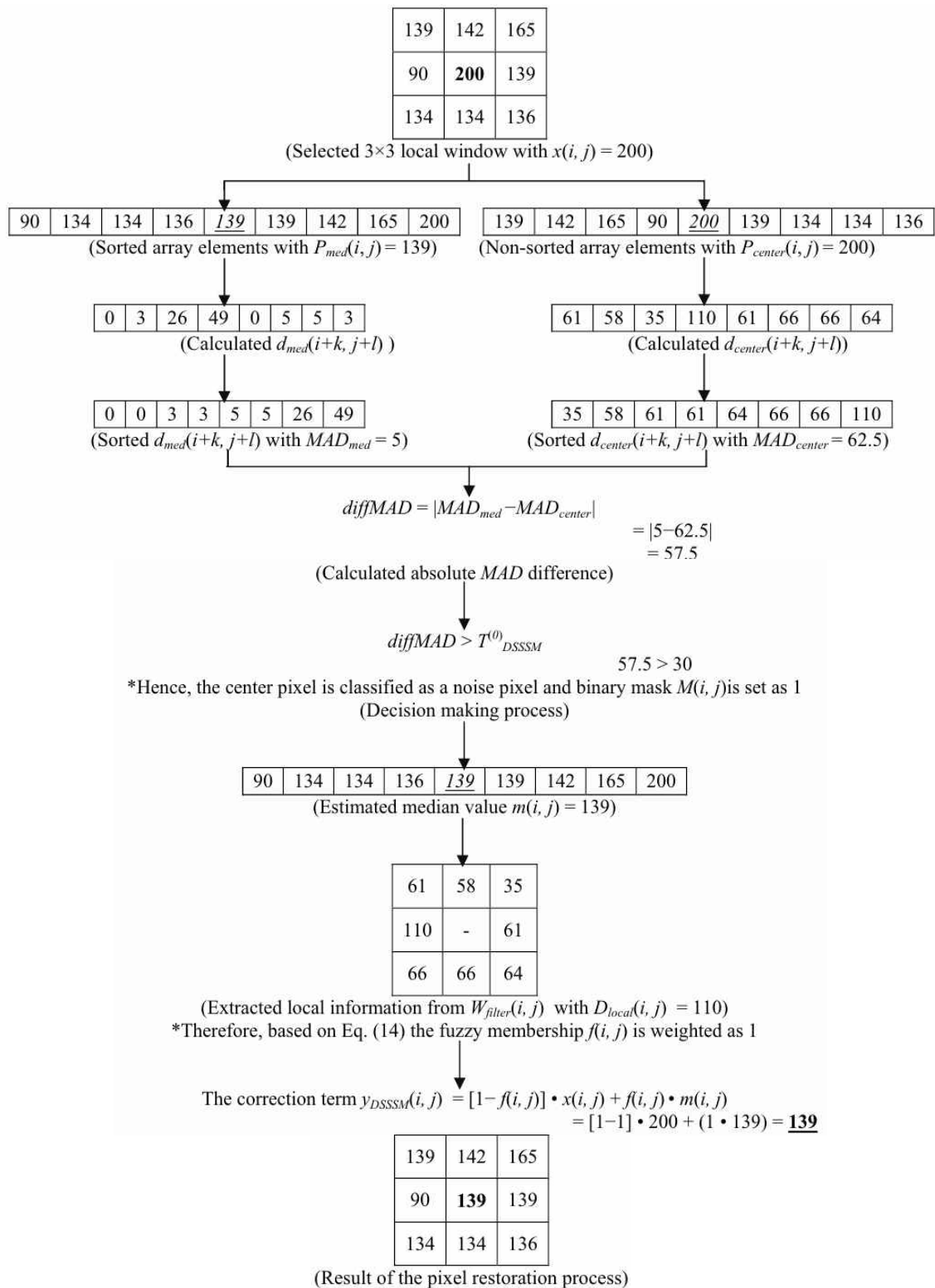


Fig. 1. The illustrated example on the DSSSM noise filtering operation

performance and efficient processing time, the suggested numbers of iterations for DSSSM filter are listed in Table 1.

From the results observed in Tables 2 to 4, the threshold sets are suggested as  $[T^{(0)}=25, T^{(1)}=15]$  for the 1% to 9% impulse noise cases,  $[T^{(0)}=30, T^{(1)}=20, T^{(2)}=15]$  for the

10% to 19% impulse noise cases and  $[T^{(0)}=35, T^{(1)}=25, T^{(2)}=20, T^{(3)}=15]$  for the 20% to 30% impulse noise cases. Noticeably, at each iteration the threshold  $T^{(l)}_{DSSSM}$  is applied in a decreasing manner. The reason in lowering  $T^{(l)}_{DSSSM}$  is to trace the remaining noise pixels which

**Table 1.** The suggested number of iterations for different noise densities

Number of Iterations	Impulse Noise Density
2	$r < 10\%$
3	$10\% \leq r < 20\%$
4	$20\% \leq r \leq 30\%$

**Table 2.** The noise filtering capabilities of DSSSM filter with different threshold set (5% noise).

Threshold $(T(0), T(1))_{DSSSM}$	Average PSNR
30,20	35.9163
25,15	<b>36.0348</b>
20,10	35.3107

**Table 3.** The noise filtering capabilities of DSSSM filter with different threshold set (10%, 15% noise).

Threshold $(T(0), T(1), T(2))_{DSSSM}$	Average PSNR (10%)	Average PSNR (15%)
40,30,25	33.8338	32.3589
30,20,15	<b>34.1875</b>	<b>33.1333</b>
25,15,10	33.7779	32.7030

**Table 4.** The noise filtering capabilities of DSSSM filter with different threshold set (20%-30% noise).

Threshold $(T(0), T(1), T(2), T(3))_{DSSSM}$	Average PSNR (20%)	Average PSNR (25%)	Average PSNR (30%)
45,35,20,25	31.094	30.111	29.128
35,25,20,15	31.927	31.059	30.166
30,20,15,10	31.580	30.733	29.770

have smaller *diffMAD*.

Meanwhile, in order to determine the optimum threshold set, five well-known test images consist of Cameraman, Pepper, Bridge, Jet and Goldhill with  $r \in [5\%, 10\%, 15\%, 20\%, 25\%, 30\%]$  have been adopted to be tested in a series of simulations using different set of threshold. The average PSNR values for each noise level are shown in Table 2, 3 and 4.

#### 4. Simulation Results and Discussion

In this section, the performance of the proposed DSSSM filter will be compared to other related state-of-the-art impulse noise filters based on their simulation results. A total of 80 standard test images of size  $512 \times 512$ , obtained from diverse online sources were used for the simulations of each implemented filters. They are selected because these test images contain fine image details and textures which are suitable to assess the strengths and weaknesses of the implemented impulse noise filters. Each of the test images was corrupted with the impulse noise model described in (1), ranging from 5% to 30% with an increment of 5%. This set of standard test images contains various characteristics which are suitable to assess the robustness of the implemented filters.

For comparison, the following conventional impulse

noise filters with their suggested tuning parameters were used to restore the contaminated test images. Among them are SWM-I ( $T_i=50$ ) [4], SWM-II ( $T_i=30, w=3$ ) [4], TSM ( $T=20, w=3$ ) [11], DWM ( $wm=2, T_0=510, N_{max}=[5, 11]$  and  $5 \times 5$  window size) [8], LUO ( $LD=1, u=3, W1=5, W2=30$ ) [13] and ACWM ( $[\delta 0, \delta 1, \delta 2, \delta 3]=[40, 25, 10, 5, s=0.6]$ ) [10]. Finally, the simulation results of the implemented impulse noise filters will be interpreted

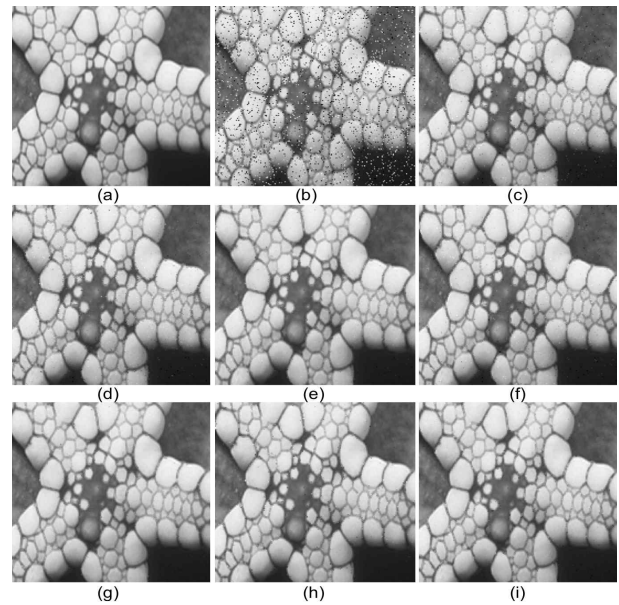


**Fig. 2.** Simulation results on a portion of *Starfish* using; (a) original image, (b) noisy image with 10% density of impulse noise, (c) SWM-I, (d) SWM-II, (e) TSM, (f) DWM, (g) LUO, (h) ACWM and (i) DSS

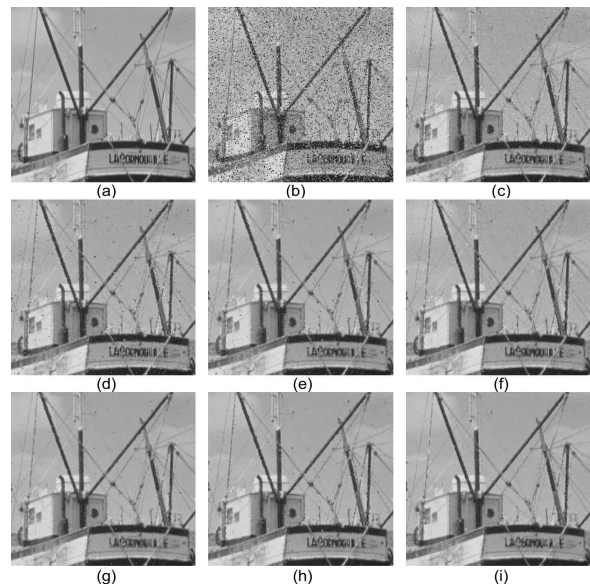


**Fig. 3.** Simulation results on a portion of *Boat* using; (a) original image, (b) noisy image with 20% density of impulse noise, (c) SWM-I, (d) SWM-II, (e) TSM, (f) DWM, (g) LUO, (h) ACWM and (i) DSSSM

objectively and subjectively as to judge the filters effectiveness in removing random-valued impulse noise.

#### 4.1 Qualitative analysis

Providing visually pleasing output is imperative, since the image is eventually to be viewed by human eye. Therefore, the appearances of the resultant images are inspected visually to judge the filters efficiencies in reducing impulse noise effect and producing good image quality. Among the 80 test images, the simulation results for three commonly used grayscale test images Starfish, Boat and Goldhill are presented in Fig. 2, Fig. 3 and Fig. 4, respectively. In each figure, portion (b) represents the noise corrupted images with 10%, 20% and 30% density of noise.

As can be seen in Starfish, at 10% impulse noise density, the noise filtering performance of DSSSM filter is basically similar to those of the conventional noise filtering algorithms. All filters are found to be able of producing perceptible reconstructed image since the density of impulse noise is still low and not form any noise patches at this level.

However, in Boat which is contaminated with 20% of impulse noise (as shown in Fig. 3), it can be visualized that the results produced by the conventional median filters are still influenced by the noise. It is able to notice that some small noise patches are remained intact on the resultant images. On contrary, the proposed DSSSM filtering algorithm can significantly remove the effect of noise added to the images and at the same time preserve the object shapes.

The similar results are obtained for the image named Goldhill; where the proposed DSSSM filtering algorithm outperforms the conventional SWM-I, SWM-II, TSM, DWM, LUO and ACWM algorithms by giving clearer filtered image even the density of noise in this image is higher (i.e. 30% of impulse noise). The proposed DSSSM filter has successfully reduced the noise particles and noise patches, consequently created less corrupted image. This observation indicates that the combination of the adaptive impulse noise detection concept with the fuzzy based local information significantly helps the proposed DSSSM filter to dexterously reduce the noise stain. Meanwhile, there is a great deal of noise contamination existed in the images produced by the conventional filtering techniques. The poor restoration results among these conventional filters can be attributed from their impulse noise filtering mechanisms which are less robust towards the contamination of random-valued impulse noise.

#### 4.2 Quantitative analysis

In addition to the visual inspection of the restored images, the quality of the restored images is also evaluated quantitatively using the peak signal-to-noise ratio (PSNR). Mathematically, the PSNR for a digital image of the dimension  $M \times N$  is defined as:

$$PSNR = 10 \log_{10} \left( \frac{255^2}{MSE} \right) (dB) \quad (16)$$

For the above formulae, MSE stands for the mean-squared error and it is given as:

$$MSE = \frac{1}{M \times N} \sum_{i=0}^{M-1} \sum_{j=0}^{N-1} [o(i, j) - y(i, j)]^2 \quad (17)$$

where  $y(i, j)$  is the filtered image and  $o(i, j)$  is the original noise-free image. Apart from the PSNR assessment, the mean of absolute error (MAE) has also been used in this analysis to characterize the filter's detail preservation behavior, one which is defined by:

$$MAE = \frac{1}{M \times N} \sum_{i=0}^{M-1} \sum_{j=0}^{N-1} |o(i, j) - y(i, j)| \quad (18)$$

The numerical results for Figs. 2(c)-(i), Figs. 3(c)-(i) and Figs. 4(c)-(i) are tabulated in Table 5. From the functions, the larger PSNR and smaller MAE values show better restoration results. In all tables, the best results obtained are made bold.

As reported in Table 5, except for the 10% impulse noise

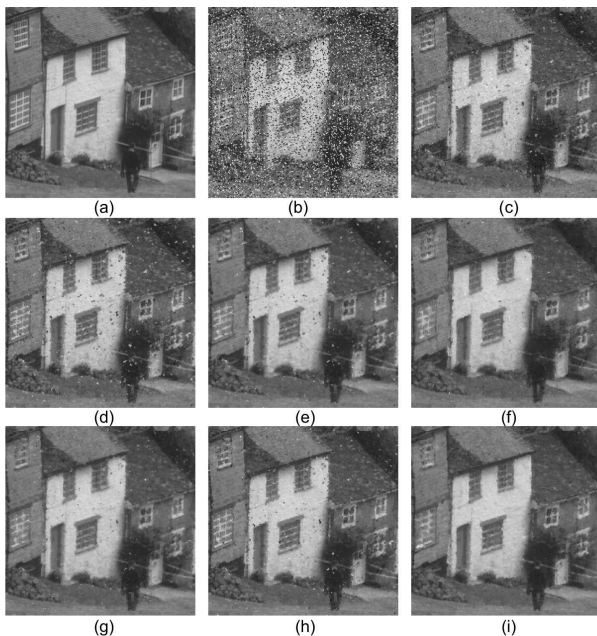


**Fig. 4.** Simulation results on a portion of *Goldhill* using: (a) original image, (b) noisy image with 30% density of impulse noise, (c) SWM-I, (d) SWM-II, (e) TSM, (f) DWM, (g) LUO, (h) ACWM and (i) DSSSM

**Table 5.** Comparison of PSNR on Different Noise Level Restoration for ‘Starfish’, ‘Boat’ and ‘Goldhill’ (Test Image)

Images	Algorithms	10%	PSNR(dB) 20%	30%
Starfish	SWM-I	31.6219	27.8273	24.7745
	SWM-II	33.056	27.8818	23.8052
	TSM	35.0013	30.2872	26.1675
	DWM	32.6523	29.6524	27.9957
	LUO	35.1372	31.4958	28.0056
	ACWM	35.3272	30.6981	26.55
	DSSSM	<b>35.3753</b>	<b>32.7072</b>	<b>30.5841</b>
Boat	SWM-I	31.1459	27.7627	24.866
	SWM-II	32.4632	28.0734	24.1192
	TSM	33.6079	30.1461	26.3557
	DWM	32.5794	29.4737	27.6844
	LUO	34.0311	31.2224	27.9866
	ACWM	<b>34.4813</b>	30.5946	26.6566
	DSSSM	34.2323	<b>31.9472</b>	<b>30.0266</b>
Goldhill	SWM-I	31.3933	27.9749	25.0891
	SWM-II	33.1147	28.4592	24.4252
	TSM	34.1815	30.6761	26.7165
	DWM	33.3963	30.0995	29.0558
	LUO	34.8439	32.0345	28.6311
	ACWM	<b>35.0158</b>	31.1301	27.0137
	DSSSM	34.4235	<b>32.4756</b>	<b>30.8526</b>

**Table 6.** Comparison of MAE on Different Noise Level Restoration for ‘Starfish’, ‘Boat’ and ‘Goldhill’ (Test Image)

Images	Algorithms	10%	MAE 20%	30%
Starfish	SWM-I	1.37569	3.01962	5.21482
	SWM-II	1.16153	2.82004	5.49509
	TSM	0.925304	2.02381	3.84945
	DWM	1.17076	2.3494	3.52177
	LUO	0.983086	1.88244	3.21782
	ACWM	<b>0.759693</b>	1.78849	3.48141
	DSSSM	0.826065	<b>1.58328</b>	<b>2.49641</b>
Boat	SWM-I	1.46273	3.05105	5.19042
	SWM-II	1.2075	2.7313	5.27398
	TSM	1.13034	2.14042	3.87268
	DWM	1.2042	2.42207	3.66792
	LUO	1.18715	2.03902	3.35503
	ACWM	<b>0.836605</b>	1.80618	3.43848
	DSSSM	0.955929	<b>1.71384</b>	<b>2.5858</b>
Goldhill	SWM-I	1.46043	3.07207	5.17048
	SWM-II	1.19814	2.73936	5.21354
	TSM	1.12705	2.1397	3.82618
	DWM	1.13602	2.33179	3.29423
	LUO	1.19761	2.03074	3.26606
	ACWM	<b>0.909317</b>	1.89498	3.5232
	DSSSM	1.01952	<b>1.77089</b>	<b>2.61645</b>

of *Boat* and *Goldhill*, the proposed DSSSM filtering technique consistently yields the highest PSNR values compared to the other existing conventional filters. Even though the PSNR values of ACWM filter in *Boat* and *Goldhill* are slightly higher than DSSSM filter when  $r = 10\%$ , but in terms of visual evaluation in Fig. 4(h) and 4(i), no significant difference between the two images are observed.

Meanwhile, the similar phenomenon is occurred in the

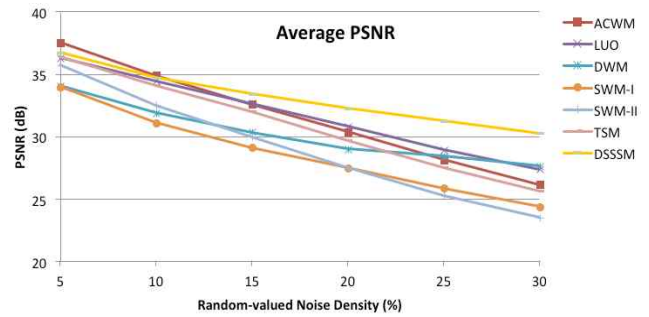


**Fig. 5.** The graph of an average PSNR based on different noise level restorations for 80 standard grayscale test images

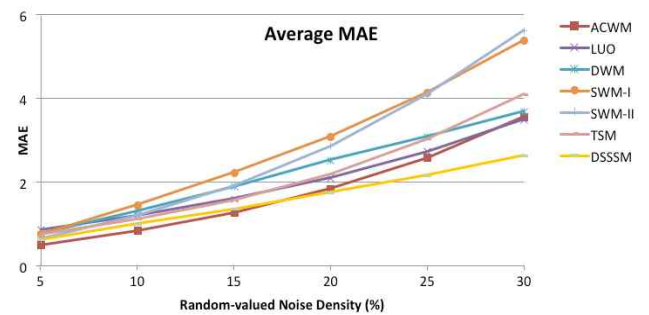


**Fig. 6.** The graph of an average MAE based on different noise level restorations for 80 standard grayscale test images

analysis outlined in Table 6, where the proposed DSSSM filter without fail outclasses the other filters in comparison by producing the best MAE results for the cases of 20% and 30% impulse noise density. These findings strongly support the qualitative results in Section 4.1. On the contrary, at 10% of impulse noise density, it can be observed that ACWM gives the better MAE results as compared to our proposed filter. However the performances of these two algorithms in terms of the details preservation based on the visual perception are fairly similar (e.g. see Fig. 2). This study has further calculated the average PSNR for 80 tested images and the results are displayed in the graph shown in Fig. 5. It could be obviously observed that, for such a mild corruption rate (i.e. noise density of 15% and above), the average PSNR curve of the proposed DSSSM filter has the highest curve as compared to the rest of the filters implemented.

In the meantime, ACWM filter initially has a relatively higher average PSNR than the DSSSM filter; but it start to drop dramatically with the increased in noise density beginning from 15% impulse noise. Above 20% impulse noise density, the two worst performing filters are the SWM-I and SWM-II filters.

In addition, Fig. 6 shows the extrapolation of the average MAE curves obtained using the various conventional filters in comparison and the proposed DSSSM filter. From the plot, it is noticed that all the filters do perform well at the

extremely low density of noise (i.e. 5% impulse noise). Nonetheless, only the proposed DSSSM filter managed to survive at all level of noise densities with the MAE is slightly and gradually increased. Other filters, such as ACWM and LUO for instance, even though are able to produce relatively good details preservation results at the beginning but their MAE values have sharply increased; particularly when the noise level is above 20%. On the other hand, the SWM-I and SWM-II filters have completely failed to compete in this test. Once again, this finding shows that the DSSSM filter is not only able to eliminate noise efficiently but it can also preserve the original appearance and shape of an image very well.

## 5. Conclusion

Throughout this study, an effective algorithm for the detection and suppression of random-valued impulse noise has been introduced. The proposed DSSSM filter is constructed by incorporating a robust impulse noise detection based on adaptive thresholding and recursive pixel restoration technique. Additionally, fuzzy reasoning set is embedded as part of the filtering mechanism in order to handle any imprecise local information. Extensive simulation results reveal that the DSSSM filter is able to reduce the random-valued impulse noise effect, while at the same time preserving the details and structures of fine images. Furthermore, its filtering performance is tremendously consistent all the time as compared to the number of well-known conventional techniques; and all these good results are achieved with a fairly efficient processing time.

## Acknowledgements

This work was supported by the Universiti Malaysia Pahang Internal Grants under grant (RDU1703151).

## References

- [1] W. Luo., "Efficient removal of impulse noise from digital images," *IEEE Trans. Consumer Electronics*, vol. 52, no. 2, pp. 523-527, 2006.
- [2] R. C. Gonzalez and R. E. Woods., "Digital image processing," New York: Addison-Wesley, 1992.
- [3] H. Hwang and R. A. Haddad., "Adaptive Median Filters: New Algorithms and Results," *IEEE Transactions on Image Processing*, vol. 4, no. 4, pp. 499-502, 1995.
- [4] T. Sun and Y. Neuvo., "Detail-Preserving Median Based Filters in Image Processing," *Pattern Recognition Letters*, 15 (1994) pp. 341-347.
- [5] T. Chen and H. R. Wu., "Space variant median filters for the restoration of impulse noise corrupted images," *IEEE Trans. on Circuits and Systems II*, 48, pp. 784-789, 2001.
- [6] S. Zhang and M. A. Karim., "A new impulse detector for switching median filters," *IEEE Signal Processing Letters*, vol. 9, no. 11, pp. 360-363, 2002.
- [7] I. Aizenberg and C. Butakoff., "Effective impulse detector based on rank-order criteria," *IEEE Signal Process. Letters*, vol. 3, no. 11, pp. 363-366, 2004.
- [8] Y. Dong and S. Xu., "A new directional weighted median filter for removal of random-valued impulse noise," *IEEE Signal Processing Letters*, vol. 14, no. 3, pp. 193-196, 2007.
- [9] H. H. Chou and L. Y. Hsu., "A noise-ranking switching filter for images with general fixed impulse noises," *Signal Processing*, 6, pp. 198-208, 2015.
- [10] T. Chen and H. R. Wu., "Adaptive impulse detection using centre-weighted median filter," *IEEE Signal Processing Letters*, vol. 8, no. 1, pp. 1-3 2001.
- [11] Chen, K. K. Ma and L. H. Chen., "Tri-state median filter for image denoising," *IEEE Transactions on Image Processing*, vol. 8, no. 12, pp. 1834-1838, 1998.
- [12] J. K. Sung, H. L. Yong., "Center weighted median filters and their applications to image enhancement," *IEEE Transactions on Circuits and Systems*, vol. 38, no. 9, pp. 984-983, 1991.
- [13] W. Luo., "An efficient algorithm for the removal of impulse noise from corrupted images," *AEU-Int. J. Electron. Commun.*, 61, pp. 551-555, 2007.
- [14] K. K. V. Toh and N. A. Mat Isa., "Cluster-based adaptive fuzzy switching median filter for universal impulse noise reduction," *IEEE Trans. Consumer Electronics*, vol. 56, no. 4, pp. 2560-2568, 2010.
- [15] <http://homepages.inf.ed.ac.uk/rbf/HIPR2/median.htm> (accessed on April 2012).
- [16] Majid, A., Lee, CH., Mahmood, M.T. et al. "Impulse noise filtering based on noise-free pixels using genetic programming," *Knowl Inf Syst* (2012) 32: p. 505.
- [17] Xu, Z., Wu, H.R., Yu, X. et al. "Adaptive progressive filter to remove impulse noise in highly corrupted color images," *SIViP* (2013) 7: p. 817.
- [18] Ilke Turkmen., "A new method to remove randomvalued impulse noise in images," *Int. J. Electron. Commun. (AEU)* 67 (2013) 771-779.
- [19] M. S. Darus, S. N. Sulaiman, I. S. Isa et al. "Modified hybrid median filter for removal of low density random-valued impulse noise in images," *IEEE International Conference on Control System, Computing and Engineering*, pp. 25-27 November 2016.
- [20] M. H Suid and N. A. M. Isa. Scientific Research and Essays, vol. 7, no. 7, pp. 813-823, 2012.



**Mohd Helmi Suid** received the B.Eng Hons in Electrical and Electronics Engineering from Universiti Teknikal Malaysia Melaka in 2007. In 2014, he received the M. Sc. from School of Electronics & Electrical Engineering, Universiti Sains Malaysia, Penang, Malaysia. He is currently, a lecturer in Faculty of Electrical and Electronics Engineering, Universiti Malaysia Pahang (UMP). His current research interests are digital image processing, vision for robotics application and computational intelligence.



**Mohd Falfazli Bin Mat Jusof** is a Lecturer in Faculty of Electrical & Electronics Engineering Universiti Malaysia Pahang. He was graduated from Ehime University, Japan for Bachelor (2008) and Master Degree (2010). His current research interests are IoT, application on embedded system, computer vision systems and physical computing.



**Mohd Ashraf Ahmad** received his first degree in B.Eng. Electrical Mechatronics and Master degree in M.Eng. Mechatronics and Automatic Control from University of Technology Malaysia (UTM) in 2006 and 2008, respectively. In 2015, he received a Ph.D in Informatics (Systems Science) from Kyoto University. Currently, he is a lecturer in Faculty of Electrical and Electronics Engineering, Universiti Malaysia Pahang (UMP). His current research interests are model-free control, control of mechatronic systems, nonlinear system identification and vibration control.